W-Band Power Combiner Design

KAI CHANG, MEMBER, IEEE, AND ROY L. EBERT

Abstract—**W-band power combiners using double-drift IMPATT silicon diodes have been developed to generate high pulsed power. The combiner design was based on a computer analysis of the cross-coupled coaxial-waveguide diode mounting structure which forms the basic module of the combiner. Peak output power of 20.5 W for a two diode combiner and 40 W for a four-diode combiner have been achieved. The diodes were operated at 100-ns pulsewidth and 0.5-percent duty cycle. The combiners demonstrated over 80-percent combining efficiency and 6-percent dc–RF conversion efficiency.**

I. Introduction

RECENT PROGRESS in the development of IMPATT devices has resulted in the generation of 13-W peak output power consistently, with 8-percent conversion efficiency at *W* band [1]. However, fundamental thermal and impedance limitations have prevented scaling these devices up to much higher power levels needed for system applications. To achieve the required high power levels, it is of great interest to incorporate several diodes in a circuit that combines the power efficiently. Many power combining approaches have been proposed and tried in the past decade. They have fallen mainly into two categories: resonant cavity combiners and nonresonant combiners. Nonresonant combiners include hybrid couplers [2] and Wilkinson-type combiners [3]–[5]. A resonant cavity combiner was first demonstrated by Kurokawa and Magalhaes [6] with a power combiner operated at *X* band using a cross-coupled coaxial-waveguide diode mounting structure as a basic module. Later, Harp and Stover [7] modified the combiner configuration by replacing the rectangular resonant waveguide cavity with a cylindrical resonant waveguide cavity. The same technique was then used by many others [8]–[10] for construction of solid-state power combiners in the microwave and lower millimeter-wave frequency range. This paper reports the state-of-the-art results of *W*-band power combiners delivering 20.5-W peak combined power for a two-diode circuit and 40 W for a four-diode circuit with over 80-percent combining efficiency. It should be emphasized that these power levels are substantially higher than the best result reported for a single diode, which is 15 W [1]. The combiner design was based on a theoretical analysis of a cross-coupled coaxial-waveguide diode mounting structure which serves as the basic module of the power combiner. This circuit model was verified by experimental measurements at lower frequencies, and the results were then applied to the combiner design in optimizing the circuit.

Manuscript received August 13, 1979; revised November 19, 1979. This work supported in part by the U.S. Army Ballistic Missile Defense Advanced Technology Center under Contract DASG60-78-C-0148.

K. Chang is with Hughes Aircraft Company, Electron Dynamics Division, Torrance, CA 90509.

R. L. Ebert was with Electron Dynamics Division, Hughes Aircraft Company, Torrance, CA 90509. He is now with TRW Defense and Space Systems Group, Redondo Beach, CA 90278.

II. Modeling of Cross-Coupled Coaxial-Waveguide Diode Mounting Structure

The cross-coupled coaxial-waveguide configuration is one of the earliest methods in providing a transition from coaxial line to waveguide [11]. In this particular application, one of the two waveguide ports and one of the two coaxial ports are short-circuited. Matching is accomplished by adjusting the lengths of the waveguide and coaxial-line short-circuited sections. Later, this method has been found undesirable for its narrow-band nature. Kenyon [12] and Magalhaes and Kurokawa [13] first constructed an IMPATT oscillator utilizing cross-coupled coaxial-waveguide structure. The IMPATT diode was mounted in a coaxial line coupled to a waveguide cavity, which in turn coupled to the load through a proper iris. A tapered absorber was attached to the other end of the coaxial line for stabilization purposes. The impedance matching to the diode was provided by adjusting the length of the coaxial section, and tuning could be accomplished by moving the sliding short at one waveguide arm. This configuration has been used very successfully for numerous applications in the design of IMPATT or Gunn oscillators and amplifiers. Many combiners also utilized this circuit as a basic module.

Although this diode mounting structure has been used extensively, the most successful use has been based primarily on empirical knowledge rather than on theoretical analysis. Lewin [14], [15] has initiated a theoretical analysis. Unfortunately, the lack of experimental verification of his study failed to establish his circuit as an accurate representation of this configuration. Eisenhart [16] established an equivalence between a coaxial entry and a gap in the post. Based on this equivalence, the coaxial-waveguide junction could be tackled by the theoretical analysis developed for waveguide-post mounting structure [17], [18]. His analysis was confirmed by experimental measurements. However, an inconvenience arises from the empirical determination of the equivalent gap, which is dependent on the waveguide aspect ratio (the ratio of waveguide width to waveguide height), post diameter, and coaxial characteristic impedance. The motivation here is to develop a computer analysis program with experimental confirmation to design the coaxial-waveguide diode

0018-9480/80/0400-0295$00.75 ©1980 IEEE

mounting structure, and to provide important information for combiner design, such as the driving-point impedance looking into the circuit at the diode plane and the power loss to the absorber located at coaxial port under different tuning and loading conditions.

The structure to be analyzed is shown in Fig. 1(a). A device, such as a Gunn diode or an IMPATT diode, can be mounted at one coaxial port while a load or a short at the other coaxial port serves as a stabilized network or a tuning element. The structures shown in Fig. 1(b) and (c) are just special cases of Fig. 1(a). Fig. 2 illustrates a general configuration of the cross-coupled coaxial-waveguide circuit. The coaxial line can be of different diameters in the upper and lower sections; and $Z1$, $Z2$, $Z3$, and $Z4$ are the load impedances at each port, respectively. The equivalent circuit shown in Fig. 3 is based on the analysis by Lewin [14] with some modifications. The inclusion of the coaxial junction capacitances suggested by Lewin was found unnecessary. The effect of phase variation of the field across the post which has been neglected in Lewin's analysis was accounted for by a lumped element [19]. The circuit elements are summarized as follows for clarity:

$$Y' = j \sum_{m=1}^{\infty} \frac{\cos m\pi}{X_m} e^{-mr\pi/b} \tag{1}$$

$$Y_{1p} = j \sum_{m=1}^{\infty} \frac{1}{X_m} e^{-m\pi r/b} - j \sum_{m=1}^{\infty} \frac{\cos m\pi}{X_m} e^{-m\pi r/b} = Y_{2p} \tag{2}$$

$$Z_{0p} = j \frac{Z_0}{4} \left[k_0^2 - \left(\frac{\pi}{a}\right)^2 \right]^{1/2} \sum_{n=2}^{\infty} \frac{\left[\cos \frac{n\pi r}{a} - \cos \frac{n\pi(2d \pm r)}{a} \right]}{\left(\frac{n^2\pi^2}{a^2} - k_0^2 \right)^{1/2}} \tag{3}$$

$$X_m = \frac{b^2}{4} \frac{\eta}{k_0 ab} \left(\frac{m^2\pi^2}{b^2} - k_0^2 \right) \left(\frac{a}{\pi} \right) [K_0(r\Gamma_m) - k_0(2d\Gamma_m)] \tag{4}$$

$$X_b = Z_0 \frac{a}{\lambda_g} \left(\frac{2\pi r}{a} \right)^2 \sin^2 \frac{\pi d}{a} \tag{5}$$

$$N = \sqrt{\csc \frac{\pi d}{a} \csc \frac{\pi(d \pm r)}{a}} \tag{6}$$

where

$$\Gamma_m = \left(\frac{m^2\pi^2}{b^2} - k_0^2 \right)^{1/2}$$

$$Z_0 = 2\eta \frac{b}{a} \frac{\lambda_g}{\lambda}$$

and

$$\lambda_g = 2\pi / \sqrt{k_0^2 - \left(\frac{\pi}{a}\right)^2}$$

$$\eta = 120\pi$$

$$k_0 = 2\pi/\lambda$$

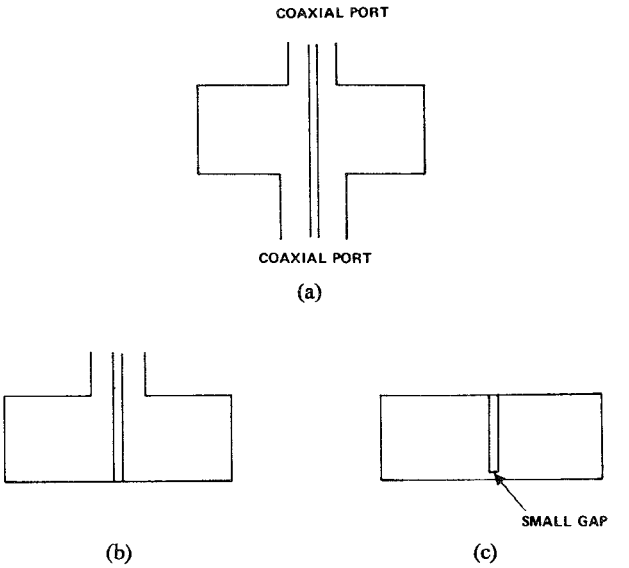

Fig. 1. (a) Coaxial-waveguide diode mounting structure. (b) Coaxial-waveguide diode mounting structure with one port shorted at the coaxial entry. (c) A waveguide post diode mounting structure with a small gap at the bottom of the post.

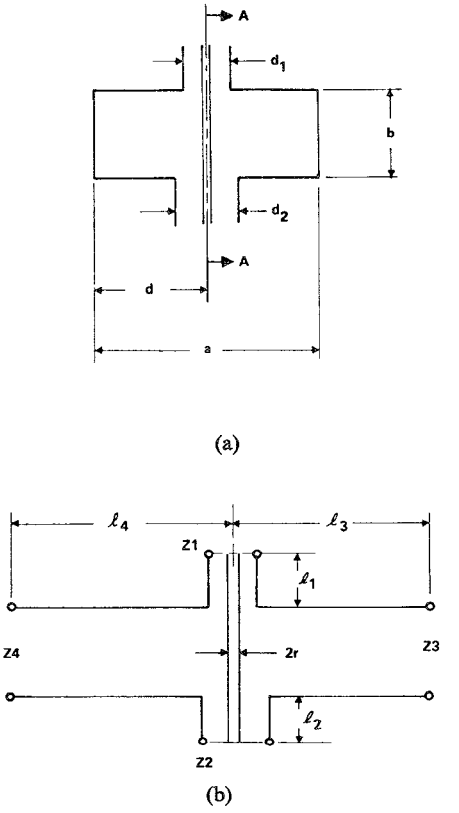

Fig. 2. (a) A coaxial-waveguide diode mounting structure. (b) Side-view on AA plane.

K_0 is the modified Bessel function of the second kind. Z_0 is the characteristic impedance of the waveguide and Z_{01} and Z_{02} are those of the coaxial lines. Z_{0p} is an inductive component due to the post in waveguide excited by TE_{n0} modes. Y' and Y_{1p}, Y_{2p} account for the effects of waveguide-coaxial junctions. This analysis is valid only

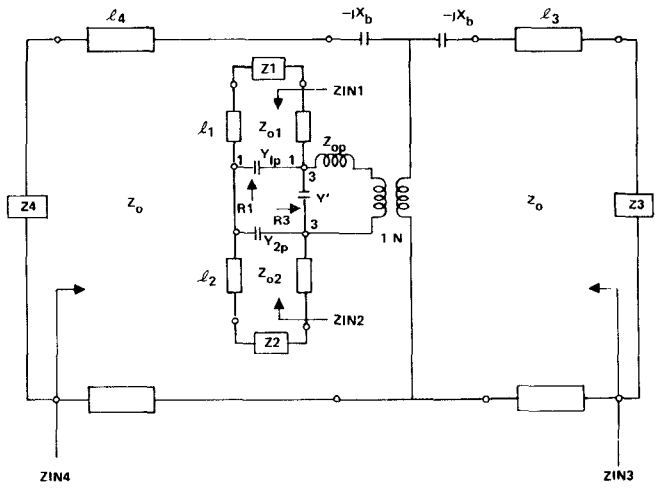

Fig. 3. Equivalent circuit of a general coaxial-waveguide diode mounting structure.

for small diameters of coax inner and outer conductor. However, it is believed that the equivalent circuit should provide approximate results even for reasonably large post and hole sizes.

*ZIN*1 is the input impedance looking into the circuit at the coaxial end with the other three ports terminated by *Z*2, *Z*3, and *Z*4. *ZIN*2, *ZIN*3, and *ZIN*4 are defined the same way, respectively. R_1 and R_3 are the real parts of the impedances looking into port 1-1 and port 3-3, as shown in Fig. 3. If an IMPATT diode is placed at *Z*2 to generate microwave power, the power generated will be split into two parts: one goes to the waveguide load and the other reaches the absorber located at *Z*1. The ratio *R* of the power, which relates to the coupling between the coaxial line section and waveguide cavity, is then equal to R_3/R_1. In Section V, techniques in the control of this power ratio will be discussed.

III. Experimental Verification of the Circuit Model

To facilitate the design, computer programs were developed based on the circuit model. The accuracy of the model has to be checked by comparing the computer results with experimental results. Experimental measurements at *W* band are difficult because of the lack of instrumentation and inadequate measurement accuracy. Data obtained at lower frequencies are thus used to verify the circuit model.

Eisenhart [18] has conducted a series of experiments using a 50-Ω 7-mm airline driving *X*-band waveguides. Figs. 4 and 5 show the comparison between his experimental results and our theoretical results. Fig. 6 shows the comparison for a special case in which one coaxial port is short-circuited at the coaxial entry. Further confirmation is shown in Figs. 7 and 8 for the driving-point impedance at a small gap [17], and for the obstacle impedance of a single post [17] which are special cases of the configuration shown in Fig. 2 and can be easily solved by our computer analysis. The general agreement between the

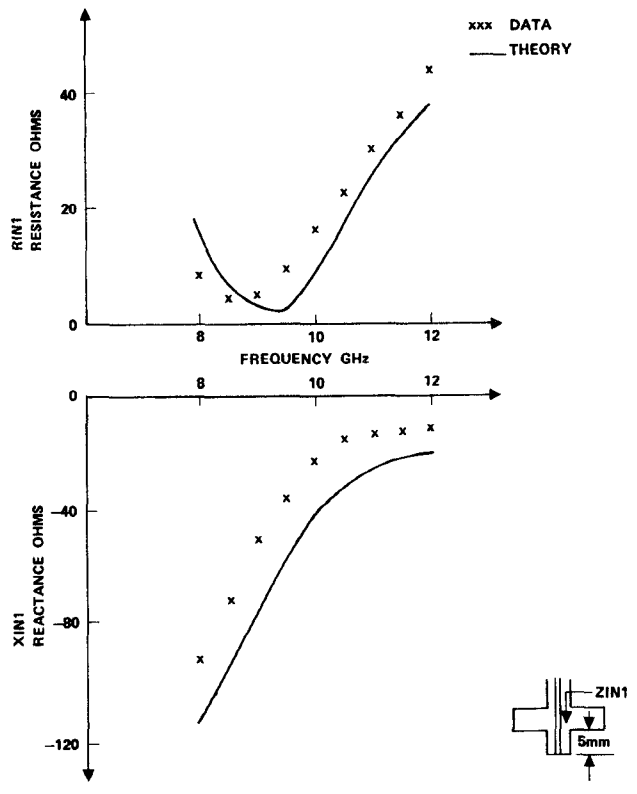

Fig. 4. Theory and experimental comparison for a 50-Ω load at coaxial port.

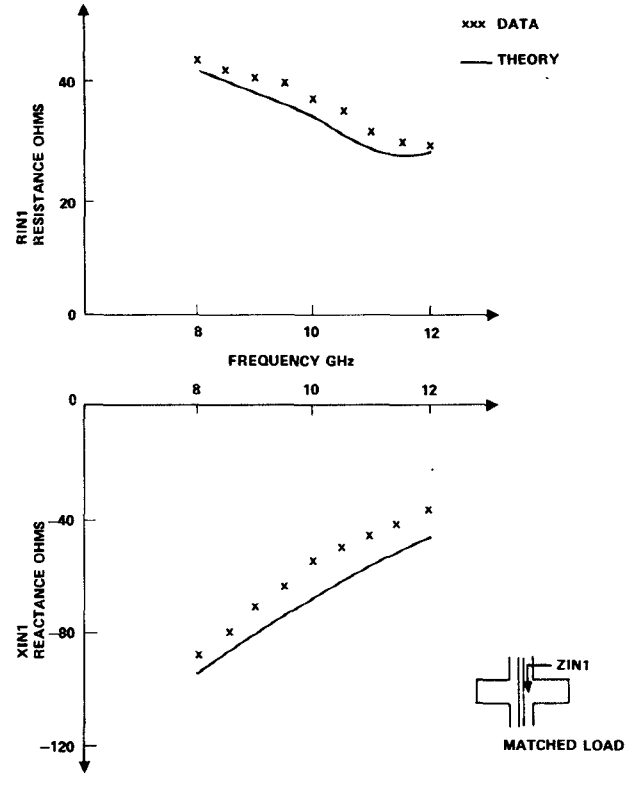

Fig. 5. Theory and experimental comparison for a short at 5 mm from the coaxial entry.

theoretical results and measurement is good. This lends considerable confidence on the circuit model and thus can be applied to our *W*-band power combiner design.

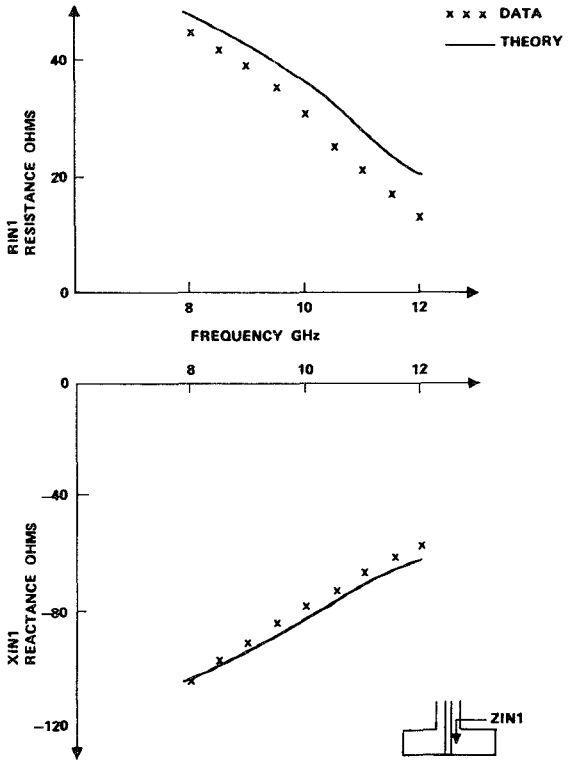

Fig. 6. Theory and experimental comparison for one coaxial port shorted at coaxial entry.

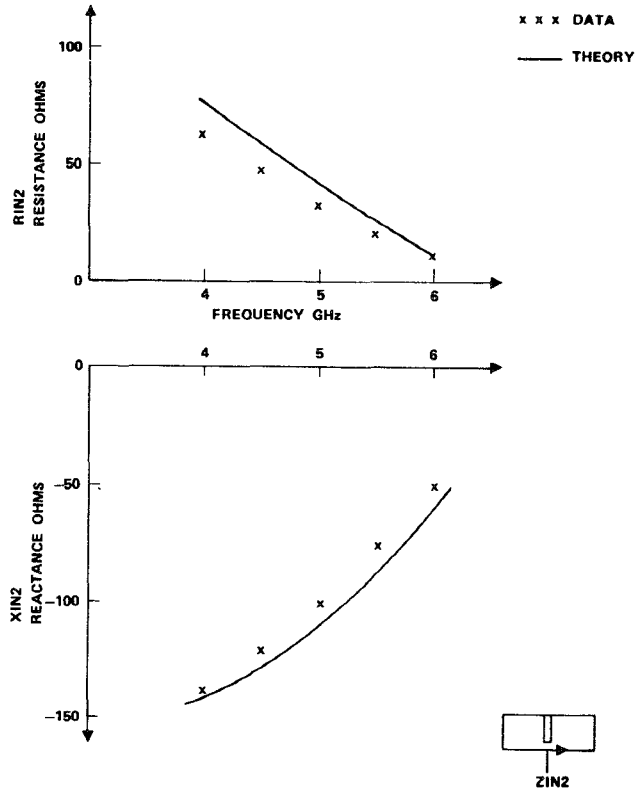

Fig. 7. Theory and experimental comparison for the driving-point impedance at the gap. The waveguide has $a=1.872$ in, $b=0.872$ in. The post is located at center with $r=0.0598$ in and the gap is small.

IV. Diode Impedance Calculations

In order to complete our design, the diode impedance has to be estimated. The silicon double-drift diode design is based on a symmetrical double-drift region, which has equal doping densities in the n and p regions. The doping density and epitaxial layer thickness were optimized using a small signal computer simulation [20]. The doping concentration was determined to be $1.3\times10^{17}/\text{cm}^3$ and the operating current density was generally over 80 kA/cm^2 for pulsed operation. The resultant small signal device admittance can be calculated and is shown in Fig. 9. It can be seen that the peak negative conductance and maximum device Q occur nearly at 94 GHz. The calculated breakdown voltage is 16 V.

The diode was packaged in a miniature package as shown in Fig. 10(a), which consists of a 0.027-in quartz ring and a crossed gold ribbon (0.001 by 0.003 in). To keep our analysis tractable, a simple lumped-element model for the package is assumed to be valid up to 100 GHz. It must be emphasized that the complexity in analyzing the millimeter-wave circuit and package precludes an exact analysis for quantitative predictions. Our objective is to understand the qualitative behavior of the device and circuit; and, more important, to identify the controlling parameters to facilitate further circuit improvement. As shown in Fig. 10(b), the package parasitics [21] are modeled by an ideal inductance L_p representing

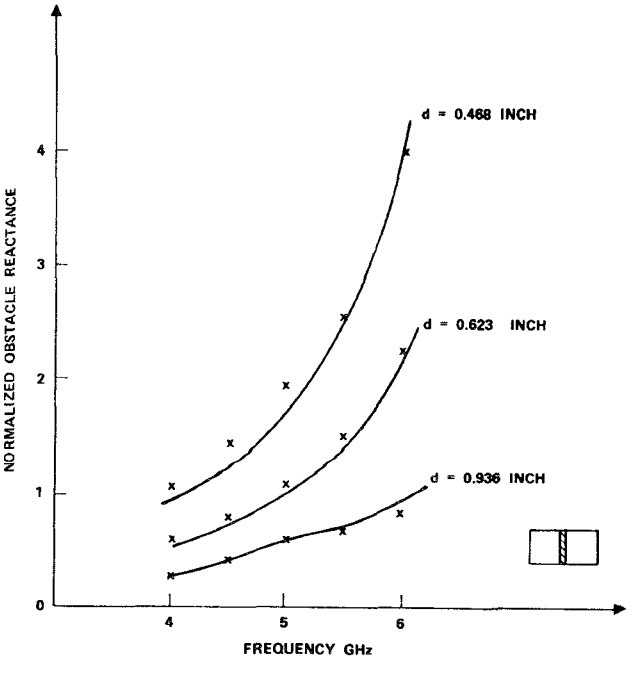

Fig. 8. Theory and experimental comparison for the normalized obstacle reactance for a single post located at different positions along the waveguide transverse direction. The following data are used: $a=1.872$ in, $b=0.872$ in, $r=0.030$ in.

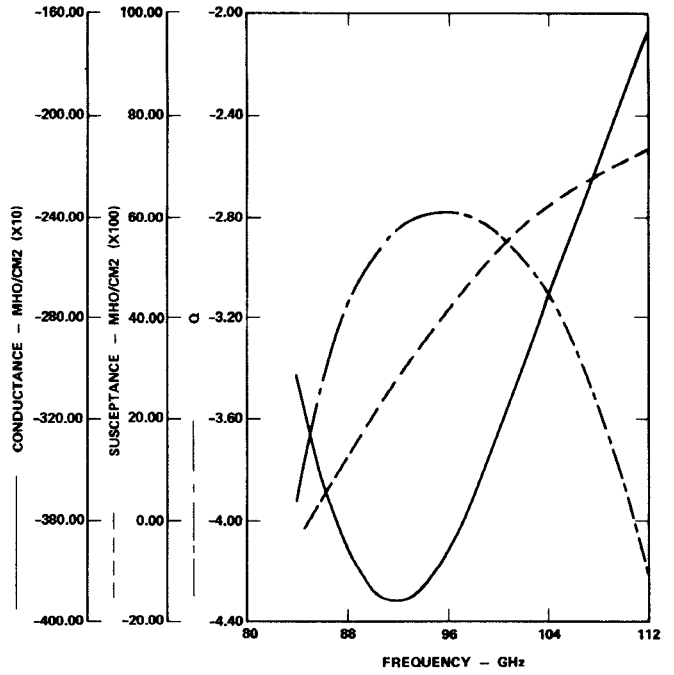

Fig. 9. Computer output of the small-signal admittance for a W-band pulsed double-drift IMPATT diode with $N_A = N_D = 1.3 \times 10^{17}$ cm^{-3}, $J = 80$ kA/cm^2, and junction temperature $T_j = 250$ °C.

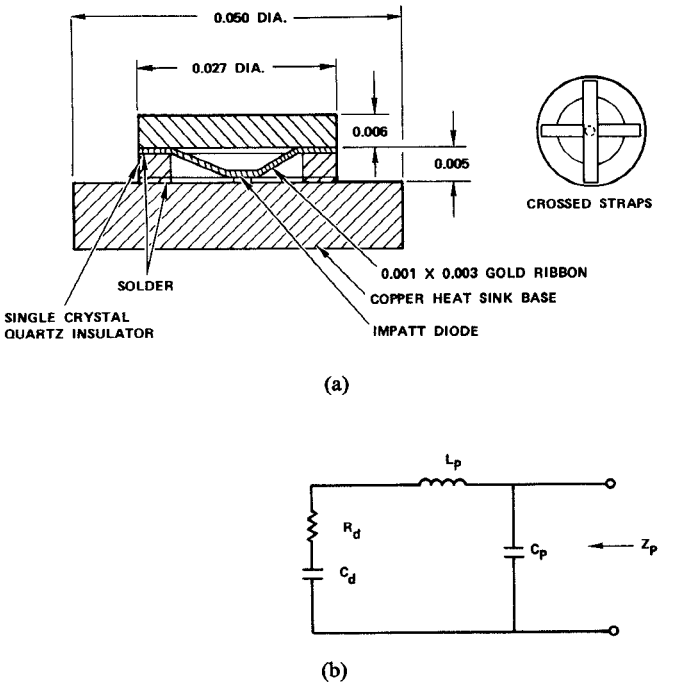

Fig. 10. Quartz ring package and its equivalent circuit designed for W-band diode. (a) Package configuration. (b) Equivalent circuit of the diode and package. All dimensions are in inches.

the gold ribbon and a capacitance C_p representing the package capacity which is largely due to the quartz ring. The element values have been characterized by measure-

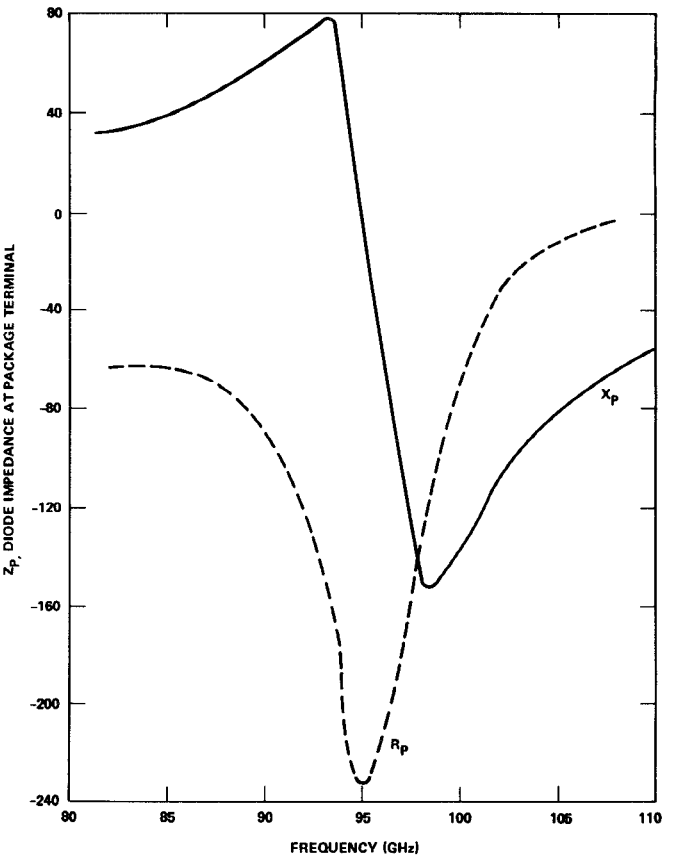

Fig. 11. Device impedance at package terminal as a function of frequency.

ments at X-band frequencies using a network analyzer. The package capacitance was found to have a value of 0.1 pF and the package inductance was 0.03 nH for the crossed strap configuration.

Using these package values and the results from small signal analysis, the device impedance at the package terminal can be calculated. For a typical 4.5-pF diode, the results are illustrated in Fig. 11 as a function of frequency. It is seen that the diode impedance has been transformed to a much higher value and a resonance occurs near 95 GHz. The diode is generally designed to be operating most efficiently at frequency near but below the package resonance frequency. Reducing package parasitics or using a smaller area diode will move the resonance to a higher frequency.

V. Design Information

The computer program developed for the circuit model was used as a design tool for the W-band power combiner. As shown in Fig. 2, there are more than fourteen parameters in the circuit model. An exact quantitative design should include interactions among posts and is thus very difficult, if not impossible. Our purpose is to determine which parameters are most critical. These highly sensitive parameters should be then designed with

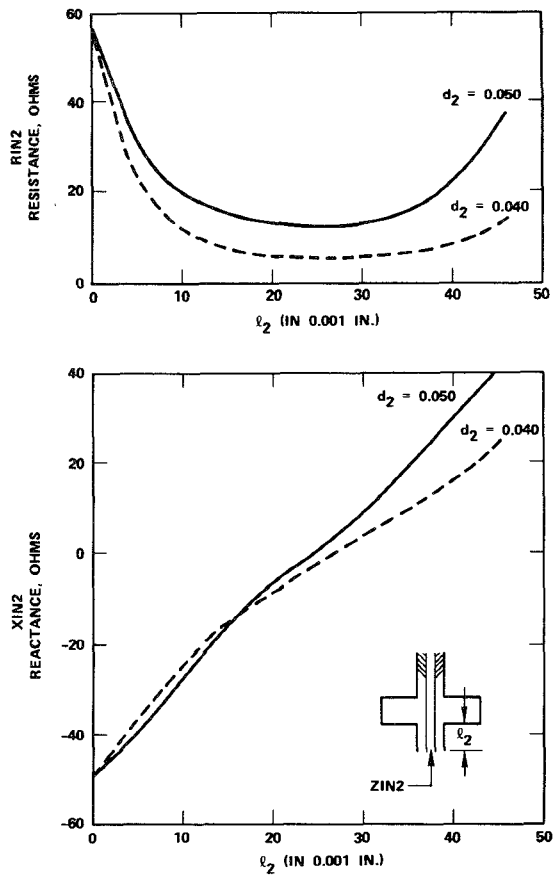

Fig. 12. Driving-point impedance looking into the circuit at the diode plane as a function of l_2 for several different hole sizes.

extreme care or made as adjustable elements. In our design, the efforts are also directed to match the circuit driving-point impedance to the diode impedance and to reduce the power dissipated in the eccosorb absorber.

Unless otherwise mentioned, consider the following parameters for our analysis of a W-band cross-coupled coaxial-waveguide circuit:

$a=0.100$ in
$b=0.030$ in
$r=0.0135$ in
$d_1=0.050$ in
$d_2=0.050$ in
$l_1=0.045$ in
$l_2=0$ in
$l_3=0.120$ in
$l_4=0.040$ in
$d=0.0175$ in
frequency = 94 GHz.

A short-circuited termination is located at $Z4$. The post is usually off-centered for the waveguide cavity power combiner. The waveguide used is a reduced-height waveguide. A full-height waveguide is connected at $Z3$ and a step transition is formed there. This step discontinuity can be calculated using the formula outlined in [22]; the results have been included in the simulation. A power ratio R is defined to indicate the amount of power delivered to the load compared to that dissipated at the stabilized circuit. The larger the value of R, the better is the efficiency. Suppose a matched load is connected to $Z1$, the driving-point impedance $ZIN2$ looking into the circuit at the diode plane is shown in Fig. 12 as a function of l_2 for different values of d_2. The oscillation occurs under the following conditions:

$$\mathrm{Im}(Z_p)+\mathrm{Im}(ZIN2)=0 \tag{7}$$

$$|\mathrm{Re}(Z_p)|>\mathrm{Re}(ZIN2) \tag{8}$$

where Re and Im denote the real and imaginary parts of a complex variable, respectively. Z_p is the device impedance at the package terminal as defined in Fig. 10(b). From Figs. 11 and 12, it can be seen that no spacer (i.e., $l_2=0$) is needed to transform the impedance levels in our combiner design. In order to match the circuit and to achieve higher power delivered to the load rather than dissipated in the absorber, one can adjust the waveguide short position at $Z4$ (i.e., a variable l_4) and insert a tuning element at $Z3$ (i.e., a variable $Z3$). The results are best illustrated in Figs. 13 and 14. It is apparent that the circuit impedance is very sensitive to the short position and external loading. Fig. 14 also indicates that the best power can be obtained without using any tuning in the output port. All these curves are derived under the assumption that a matched load is attached to $Z1$. In practice, an eccosorb absorber material is placed at $Z1$ and its impedance is difficult to evaluate at W band. To investigate the effects of the eccosorb absorber, two values of $Z1$ are used to generate the impedance and power ratio as a function of absorber position. Fig. 15 shows that the circuit impedance $ZIN2$ is not quite sensitive to $Z1$, but the power ratio varies drastically with the position of a mismatched load. It also indicates that the mismatched load (i.e., flat type eccosorb termination) has the advantage of achieving higher output power to the external load and gives one more degree of freedom of tuning the circuit. This provides capability of individual tuning for each diode to accommodate the differences among the diodes. Also, the tuning is essential for the impedance matching from diode to circuit. With proper adjustment on eccosorb positions, the power dissipated in eccosorb can be reduced to a minimum.

In summary, the circuit analysis has been used to establish the design of the W-band power combiner. It was found that no coaxial section is needed to transform the diode impedance to the waveguide cavity. Results also indicated that eccosorb positions (at $Z1$), cavity output loading and the sliding short position are key parameters to the achievement of efficient power accumulation. Selections of waveguide height and diode separation distance are also important. In the next sections, two-diode and four-diode power combiner will be developed based on this analysis.

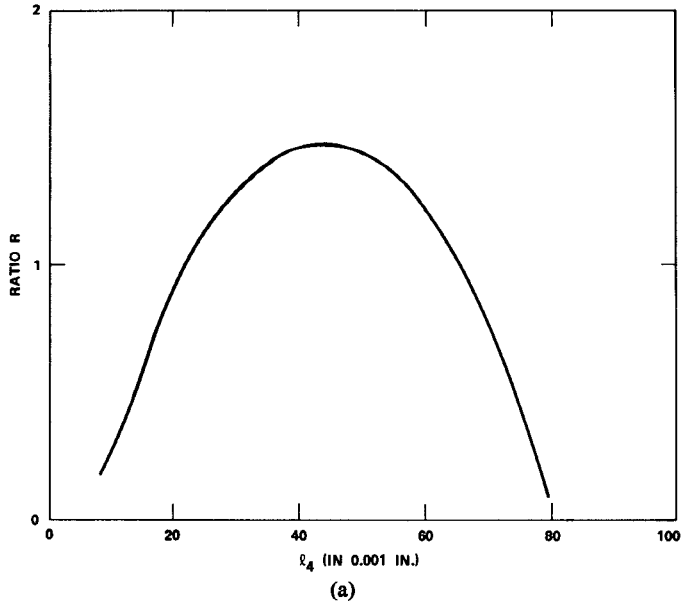

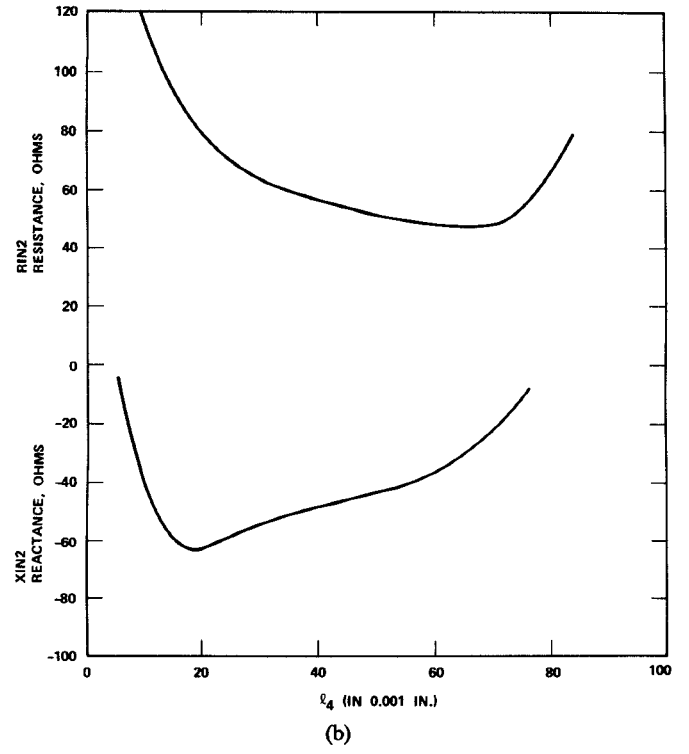

Fig. 13. *ZIN*2 and *R* as a function of l_4. (a) Driving-point impedance. (b) Power ratio *R*.

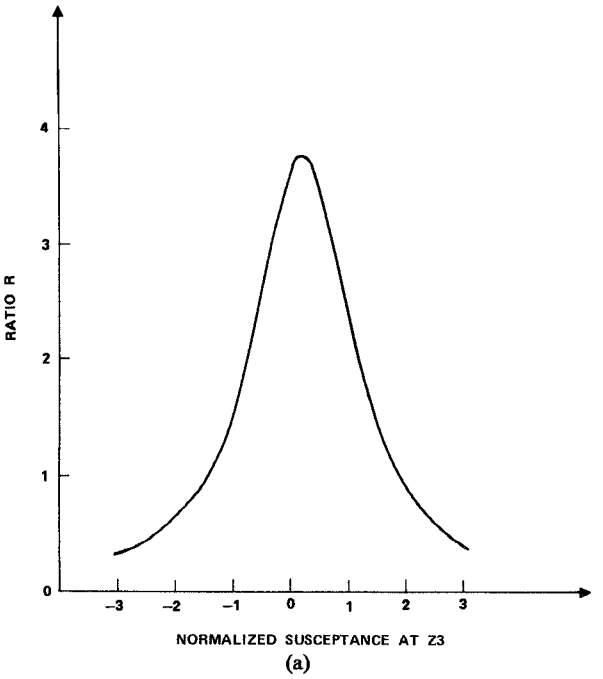

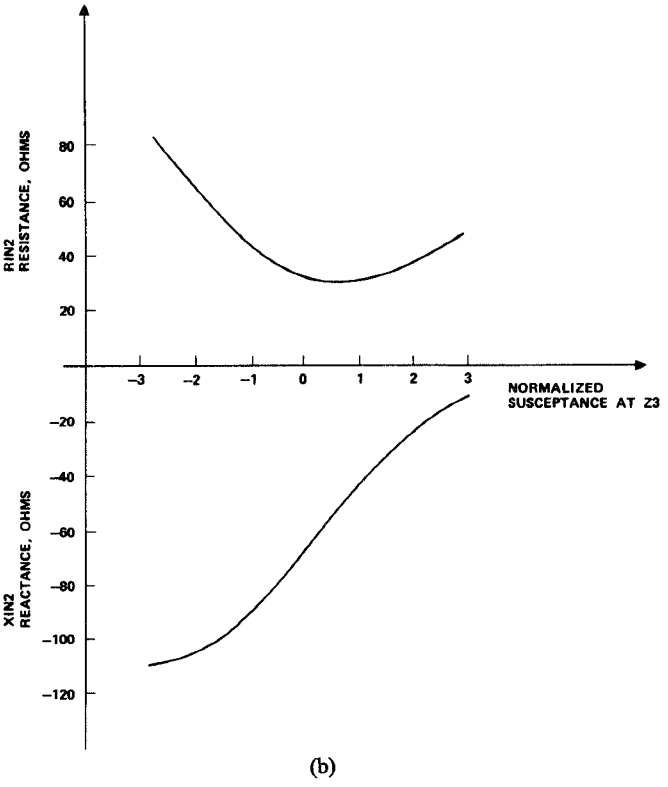

Fig. 14. *ZIN*2 and *R* as a function of loading susceptance located at 0.250 in from the post. (a) Driving-point impedance. (b) Power ratio *R*.

VI. Two-Diode Power Combiner

A two-diode power combiner [23] was designed based on the computer analysis. The cavity structure is shown in Fig. 16. As discussed in the last section, the eccosorb absorber positions and sliding short position are very crucial and thus were designed to be adjustable. Flat type eccosorb terminations were chosen for an additional degree of freedom in tuning the circuit. A tuning screw was found unnecessary if the eccosorb absorber positions were well optimized. As mentioned before, no coaxial section is needed for diode impedance transformation and the diodes were mounted on the waveguide floor. The rest of dimensions were chosen as follows based on the computer

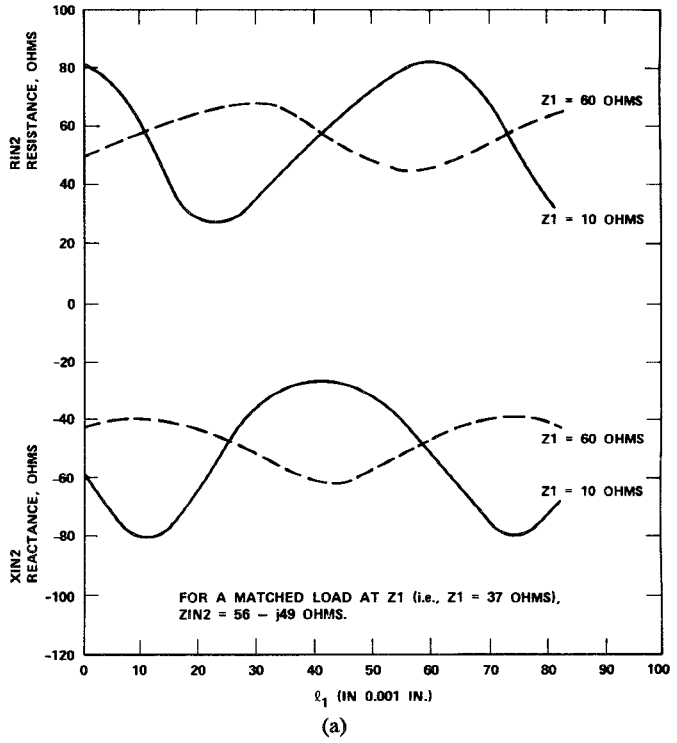

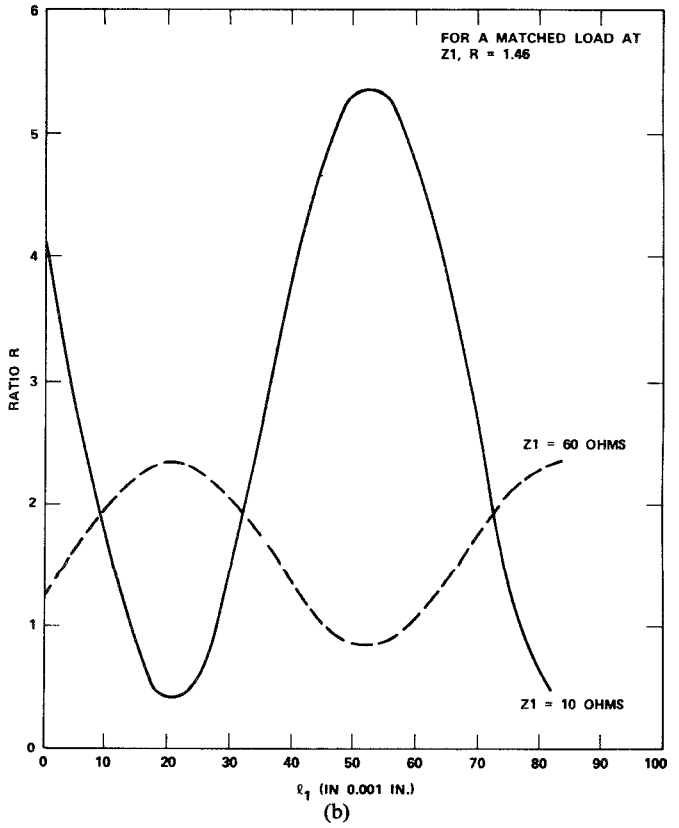

Fig. 15. *ZIN*2 and *R* as a function of l_1 for different terminations at *Z*1. (a) Driving-point impedance. (b) Power ratio *R*.

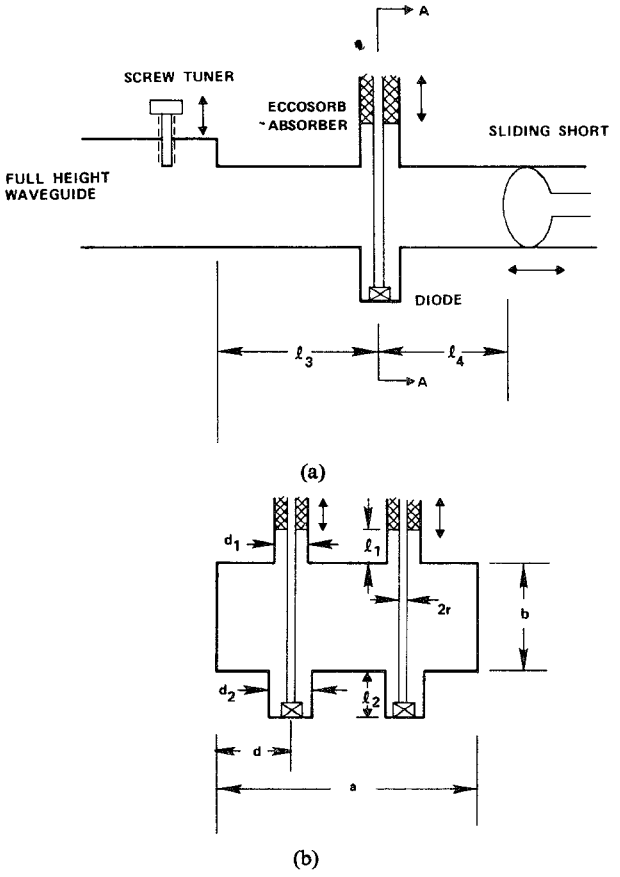

Fig. 16. Two-diode combiner waveguide cavity. (a) Side view. (b) Cross-sectional view at *AA*.

analysis:

$a = 0.100$ in
$b = 0.030$ in
$r = 0.0135$ in
$d_1 = 0.052$ in
$l_3 = 0.120$ in
$d = 0.0175$ in.

The two diodes to be combined were first individually tested in a single-diode oscillator circuit and provided 12.1 W and 12.8 W, respectively. The diodes were operated with 100-ns pulsewidth and 0.5-percent duty cycle. In the combiner, a combined peak power of 20.5 W at center frequency 92.4 GHz was achieved, and the combining efficiency was over 80 percent. Frequency chirp of less than 1 GHz and power variation across the pulse of less than 1 dB were achieved. A photograph of a disassembled waveguide circuit is shown in Fig. 17(a) and the RF-output video pulse is shown in Fig. 17(b).

VII. Four-Diode Power Combiner

In order to further increase the output power, four diodes were combined in the waveguide cavity shown in Fig. 18. The same adjustable elements designed for the two-diode combiner were also used for the four-diode

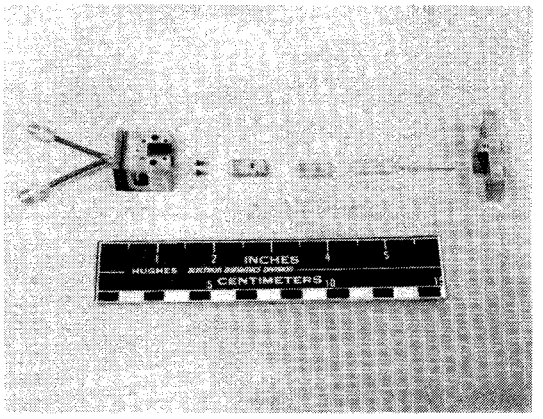

(a)

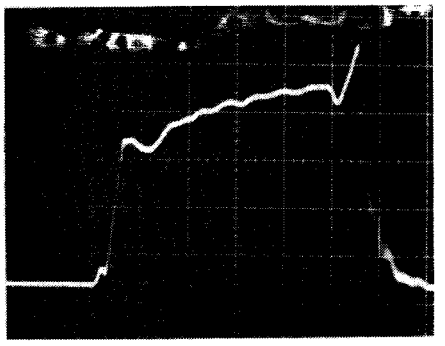

(b)

Fig. 17. Two-diode power combiner. (a) Disassembled waveguide circuit. (b) Oscilloscope display of RF-video pulse. Horizontal: 20 ns/div.

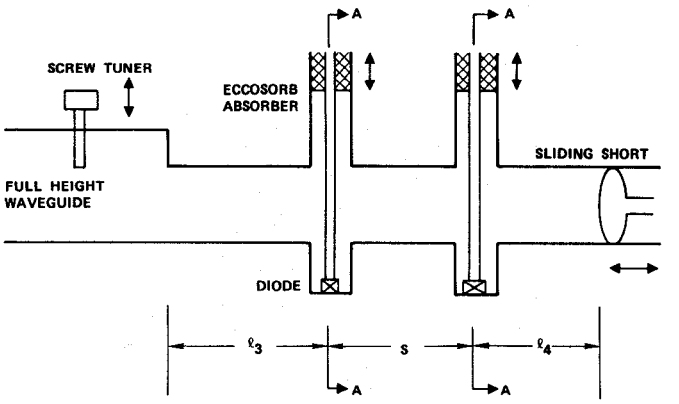

(a)

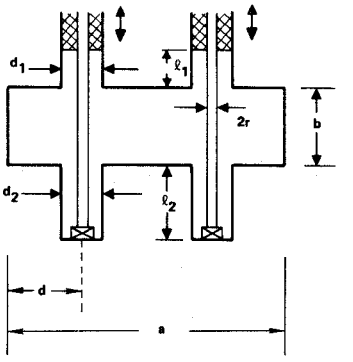

(b)

Fig. 18. Four-diode combiner waveguide cavity. (a) Side view. (b) Cross-sectional view at AA.

combiner. The dimensions are listed for clarity:

$a = 0.100$ in
$b = 0.030$ in
$r = 0.010$ in
$d_1 = 0.052$ in
$l_3 = 0.120$ in
$d = 0.019$ in
$s = 0.080$ in.

Most dimensions used here are exactly the same as the two-diode combiner cavity. The post diameter was reduced from the empirical finding that the smaller post helps the noise performance. The loading effects of one row of diodes on the other row are very difficult to assess and result in lowering the combined operating frequency. Shifting the posts to the waveguide center generally raises the operating frequency slightly. Another way to raise the frequency is to increase the package resonance frequency by redesigning the diode package.

The four diodes, which individually delivered 10–13 W in a single diode test circuit, were combined to generate 40 W at center frequency around 91 GHz with less than 1-GHz frequency chirp. The diodes were operated at 100-ns pulsewidth and 0.5-percent duty cycle. Photographs of the four-diode combiner are shown in Figs. 19(a) and 19(b) and the RF-output video pulse in Fig. 19(c). To improve the quality of bias current waveform, careful design on the bias circuit is essential. Stray capacitances should be reduced and the cable length should be kept as short as possible. A microstrip bias board has been designed and fabricated, so that four bias pulses generated from modulators can be connected to the four corners of the board and transmitted to the center through 50-Ω microstrip lines. Four bias pins are then connected to the center to pick up each individual bias pulse. As aforementioned, one can change the diode package to increase the package resonance frequency and to compensate the loading effects. By trimming the quartz ring of the diode package to reduce the parasitic capacitance, 36 W at center frequency of 93.9 GHz with 700-MHz frequency chirp has been achieved. The combiner was operated at over 80-percent combining efficiency and about 6-percent dc–RF efficiency. This power level is believed to be the highest power ever reported in W band from solid-state devices.

Because of the high circuit Q of the resonator, the mechanical tuning range of the combiner is very narrow. Typical results are shown in Fig. 20. The tuning was achieved by moving the short to selected positions and adjusting the eccosorb absorbers to maximize the output power.

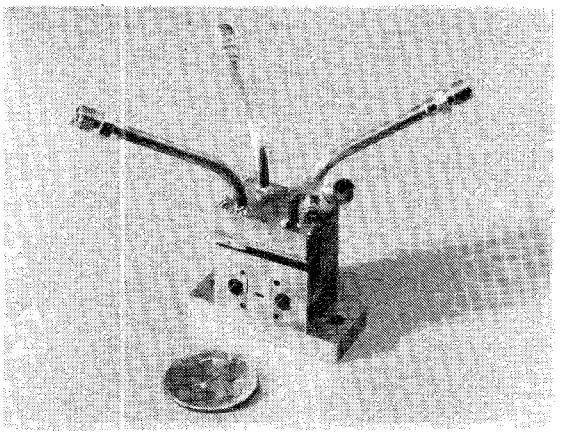

(a)

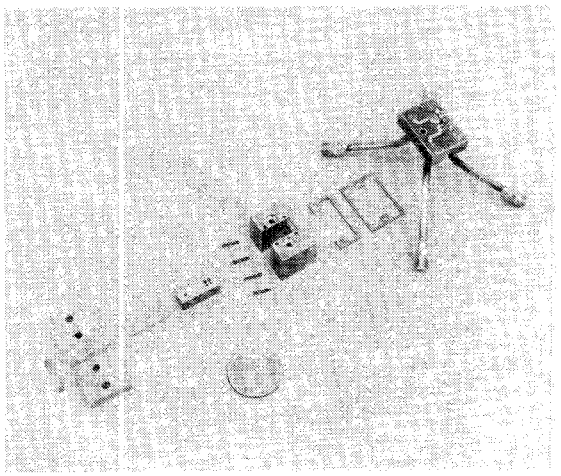

(b)

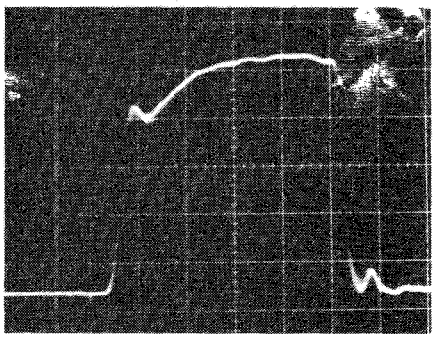

(c)

Fig. 19. Four-diode power combiner. (a) Assembled waveguide circuit. (b) Disassembled waveguide circuit. (c) Oscilloscope display of RF-video pulse. Horizontal: 20 ns/div.

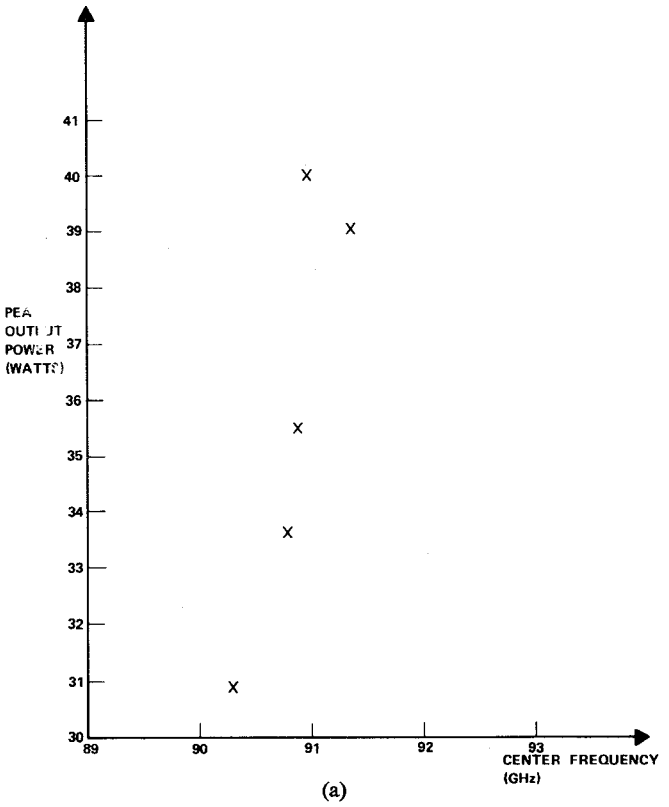

(a)

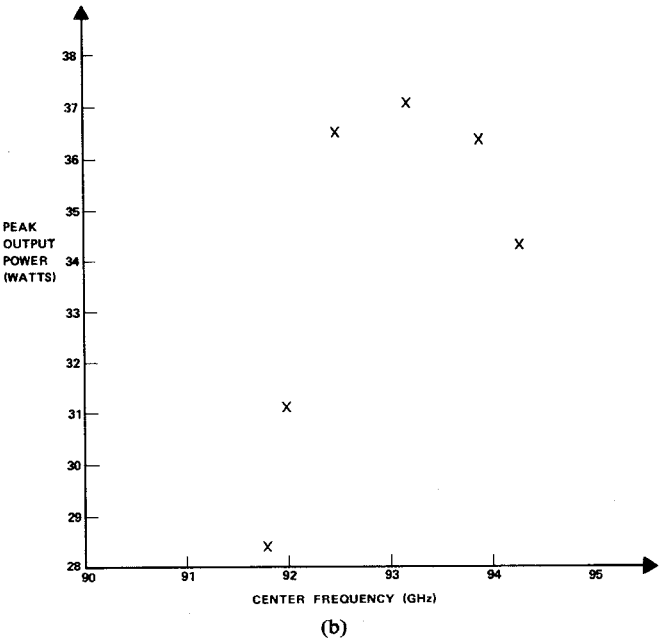

(b)

Fig. 20. (a) Tuning range for four-diode combiner. (b) Tuning range for four-diode combiner after trimming the diodes.

VII. Conclusions

W-band power combiners using double-drift IMPATT silicon diode have been developed. The combiner uses cross-coupled coaxial-waveguide diode mounting structure as a basic module. A computer analysis has been developed to optimize the circuit and the results were verified with experimental measurements at lower frequencies. The state-of-the-art results of 20.5 W from the two-diode combiner and 40 W from the four-diode combiner with over 80-percent combining efficiency and 6-percent conversion efficiency have been achieved in *W* band. The design presented here can be extended to combiners with more than four diodes.

Acknowledgment

The authors wish to thank Dr. C. Sun, Dr. T. T. Fong, and Dr. H. J. Kuno for helpful suggestions and discussions, and Dr. E. M. Nakaji for device fabrication.

REFERENCES

[1] K. Chang *et al.*, "High power 94 GHz pulsed IMPATT Oscillators," in *1979 IEEE-MTT-S Microwave Symp. Dig. Tech. Papers,* pp. 72–72, May 1979.

[2] H. J. Kuno and D. L. English, "Millimeter-wave IMPATT power amplifier/combiner," *IEEE Trans. Microwave Theory Tech.,* vol. MTT-24, pp. 758–767, Nov. 1976.

[3] C. T. Rucker, "A multiple-diode high-average-power avalanche diode oscillator," *IEEE Trans. Microwave Theory Tech.,* vol. MTT-17, pp. 553–555, Dec. 1969.

[4] J. P. Quine, J. G. McMullen, and D. D. Khandelwal, "*Ku*-Band IMPATT amplifiers and power combiners," in *1978 IEEE-MIT Microwave Symp. Dig. Tech. Papers,* pp. 346–348, June 1978.

[5] E. J. Wilkinson, "An *N*-way hybrid power divider," *IRE Trans. Microwave Theory Tech.,* vol. MTT-8, pp. 116–118, Jan. 1960.

[6] K. Kurokawa and F. M. Magalhaes, "An *X*-band 10-watt multiple-IMPATT oscillator," *Proc. IEEE,* vol. 59, pp. 102–103, Jan. 1971.

[7] R. S. Harp and H. L. Stover, "Power combining of *X*-band IMPATT circuit modules," in *1973 IEEE-ISSCC Dig. Tech. Papers,* vol. XVI, pp. 118–119, Feb. 1973.

[8] R. N. Wallace, M. G. Adlerstein, and S. R. Steele, "A 60-W CW solid-state oscillator at *C*-band," *IEEE Trans. Microwave Theory Tech.,* vol. MTT-24, pp. 483–485, July 1976.

[9] F. J. Bayuk and J. E. Raue, "*Ka*-band solid state power combiner," in *1977 IEEE Microwave Symp. Dig. Tech. Papers,* pp. 29–31, June 1977.

[10] M. Dydyk, "Efficient power combining," in *1979 IEEE Microwave Symp. Dig. Tech. Papers,* pp. 309–310, May 1979.

[11] G. L. Ragan, *Microwave Transmission Circuits,* vol. 9 (MIT Radiation Lab. Series). New York: McGraw-Hill, 1948.

[12] N. D. Kenyon, "A circuit design for *MM*-wave IMPATT oscillators," in *1970 IEEE-MIT Microwave Symp. Dig. Tech. Papers,* pp. 300–303, May 1970.

[13] F. M. Magalhaes and K. Kurkowa, "A single-tuned oscillator for IMPATT characterization," *Proc. IEEE* (Lett.), vol. 58, pp. 831–832, May 1970.

[14] L. Lewin, "A contribution to the theory of probes in waveguides," *Proc. Inst. Elec. Eng.,* Monogr. 259R, pp. 109–116, Oct. 1957.

[15] ——, *Theory of Waveguides.* New York: Wiley 1975, Ch. 5.

[16] R. L. Eisenhart *et al.*, "A useful equivalence for a coaxial-waveguide junction," *IEEE Trans. Microwave Theory Tech.,* vol. MTT-26, pp. 172–174, Mar. 1978.

[17] R. L. Eisenhart and P. J. Khan, "Theoretical and experimental analysis of a waveguide mounting structure," *IEEE Trans. Microwave theory tech.,* vol. MTT-19 pp. 706–719, Aug. 1971.

[18] R. L. Eisenhart, "Discussion of a 2-gap waveguide mount," *IEEE Trans. Microwave Theory Tech.,* vol. MTT-24, pp. 987–990, Dec. 1976.

[19] M. Marcuvitz, *Waveguide Handbook.* New York: McGraw-Hill, 1951.

[20] T. Misawa, "Negative resistance in p-n junction under avalanche breakdown conditions, Pts. I and II," *IEEE Trans. Electron Devices,* vol. ED-13, pp. 137–151, Jan. 1966.

[21] T. T. Fong, K. P. Weller, and D. L. English, "Circuit Characterization of *V*-band IMPATT oscillators and amplifiers," *IEEE Trans. Microwave Theory Tech.,* vol. MTT-24, pp. 752–758, Nov. 1976.

[22] G. L. Matthaei, L. Young, and E. M. T. Jones, *Microwave Filters, Impedance-Matching Networks and Coupling Structures.* New York: McGraw-Hill, 1964.

[23] K. Chang, R. Ebert, and C. Sun, "*W*-band two-diode power combiner," *Electron. Lett.,* vol. 15, no. 13, pp. 403–405, June 21, 1979.

Study of the Harmonic Effects for Waveguide Gunn-Diode Oscillator Optimization

EZIO M. BASTIDA, MEMBER, IEEE

Abstract—**The dependence on harmonic load conditions of waveguide Gunn oscillator performance is theoretically and experimentally studied. A simple waveguide mount is presented, which by controlling the diode harmonic load conditions, with one single adjustment permits considerable simultaneous improvement in output power, bias tuning, and varactor tuning linearities, as well as in frequency stability with the temperature. The oscillator noise level can also be minimized, though not at the same time as the other improvements. Finally, the usefulness of harmonic control in simplifying some typical thermal procedures is shown.**

I. INTRODUCTION

FOR SOME YEARS waveguide Gunn-diode oscillators have played an important role as tunable microwave sources. This is due not only to their electrical properties but also to the fact that they can be very easily constructed. Their electromagnetic behavior, however, is remarkably complex and for this reason a great deal of attention has been devoted [1]–[5] to the synthesizing of oscillator equivalent circuits. The possibility of obtaining high power, efficient electronic tuning, a low FM noise level, and a good frequency stability with the temperature is, however, often affected by some nonlinear harmonic effects that are usually not considered in oscillator models. This work first presents a survey of the effects that limit oscillator power and FM–AFC performance. An analysis of the reasons for these limits allows us to bring out interesting properties of oscillator electronic tuning and to predict a nonnegligible effect of the diode harmonic load conditions on the oscillator frequency stability with temperature and on the FM noise level. Circuit requirements for overcoming the demonstrated limits are then discussed, and a Gunn-diode waveguide mounting that satisfies the requirements is described. Finally, experimental results obtained by using the mount are presented.

Manuscript received July 25, 1979; revised November 19, 1979.

The author is with the Centro Informazioni Studi Esperienze, CISE—P.O. Box 3986, 20100, Milano, Italy.

0018-9480/80/0400-0305$00.75 ©1980 IEEE